New Journal of Physics
The open access journal for physics

Fluctuations and differential contraction during regeneration of *Hydra vulgaris* tissue toroids*

Michael Krahe[1], Iris Wenzel[1], Kao-Nung Lin[1], Julia Fischer[1], Joseph Goldmann[2], Markus Kästner[2] and Claus Fütterer[1,3,4]

[1] Fakultät für Physik und Geowissenschaften, Institut für Experimentelle Physik I, Universität Leipzig, D-04103 Leipzig, Germany
[2] Fakultät Maschinenwesen, Institut für Festkörpermechanik, Technische Universität Dresden, D-01062 Dresden, Germany
[3] Translationszentrum für Regenerative Medizin (TRM), Universität Leipzig, D-04103 Leipzig, Germany
E-mail: c.fuetterer@biophysik.net

New Journal of Physics **15** (2013) 035004 (18pp)
Received 2 July 2012
Published 4 March 2013
Online at http://www.njp.org/
doi:10.1088/1367-2630/15/3/035004

Abstract. We studied regenerating bilayered tissue toroids dissected from *Hydra vulgaris* polyps and relate our macroscopic observations to the dynamics of force-generating mesoscopic cytoskeletal structures. Tissue fragments undergo a specific toroid–spheroid folding process leading to complete regeneration towards a new organism. The time scale of folding is too fast for biochemical signalling or morphogenetic gradients, which forced us to assume purely mechanical self-organization. The initial pattern selection dynamics was studied by embedding toroids into hydro-gels, allowing us to observe the deformation modes over longer periods of time. We found increasing mechanical fluctuations which break the toroidal symmetry, and discuss the evolution of their power spectra for various gel stiffnesses. Our observations are related to single-cell studies which explain the mechanical feasibility of the folding process. In addition, we observed switching of cells from a tissue bound to a migrating state after folding failure as well as in tissue injury. We found a supra-cellular

* This paper is dedicated to Malcolm Steinberg.
[4] Author to whom any correspondence should be addressed.

actin ring assembled along the toroid's inner edge. Its contraction can lead to the observed folding dynamics as we could confirm by finite element simulations. This actin ring in the inner cell layer is assembled by myosin-driven length fluctuations of supra-cellular F-actin bundles (myonemes) in the outer cell layer.

Contents

1. Introduction

Regeneration and growth of tissues have been investigated mainly on two scales, the macroscopic one, where the tissue is considered as a piece of continuous material, and the molecular one, where tissue dynamics is reduced to biochemical signalling. The impressive recent results of cellular and molecular biophysics, however, have revealed a surprising complexity of the cytoskeletal dynamics. The question of what this complexity is required for may be partially answered by the living conditions of cells in a collective environment. However, the findings about single cells have been integrated into the picture only rudimentarily so far. We try to close the gap and investigate physical phenomena at a mesoscopic level by combining a minimum of sub-cellular and molecular structures with a coarse-grained description, e.g. as a solid or fluid, in order to explain our experimental findings. However, this field is still in its very infancy and many questions remain to be investigated.

Our multi-cellular system of choice is the cnidarian *Hydra vulgaris*. It displays a simple and uniform morphology (see figure 1(a)) and possesses only a small number of cell types. In contrast to many other multi-cellular organisms, signs of ageing could not be stated, so 'eternal life' was accorded to this organism [1]. Its reproduction and regeneration capabilities are stunning: Hydra cell assemblies and fragments prove to survive and even regenerate completely. The absence of tissue degradation and decomposition avoids misleading results. These properties, together with fast proliferation, render Hydra an ideal model organism for research on bio-mechanics and pattern formation in tissues.

Hydra inspired Alan Turing [5] to his seminal reaction–diffusion principle and, indeed, numerous grafting experiments [2–4] could be interpreted by postulating local activator and global inhibitor gradients, as proposed by him and elaborated by Gierer and Meinhardt [6, 7]. Despite great success (e.g. explanation of the existence of a minimal tissue size for regeneration), the gradient-forming molecules have still not been clearly identified [8]. Further, a diffusion mechanism across or outside of the tissue as required for building such gradients would hardly be precise and stable enough to control the observed patterning. Unfortunately,

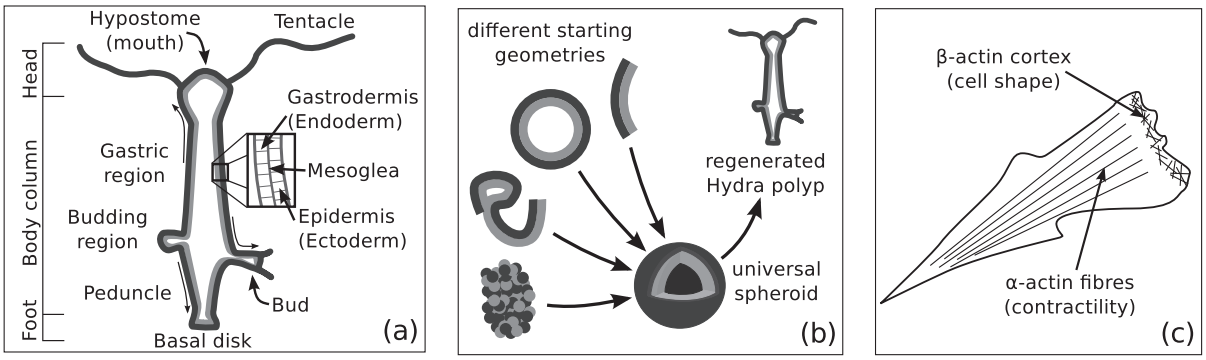

Figure 1. (a) Cross-section of a Hydra polyp with two buds. Hydra consists of two cell layers, the gastrodermis and the epidermis (also called the endoderm and the ectoderm), attached to an extracellular matrix called mesoglea. The polyp forms a tube of which one end is surrounded by 7–12 tentacles with the hypostome (mouth) in the centre while the other end (basal disc) is used to attach to surfaces. (b) Tissue fragments and cellular aggregates of different geometries first transform into the universal spheroidal geometry prior to the regeneration of a new polyp. (c) Hydra possesses two different isoforms of actin: α-actin which can build up super-cellular structures and β-actin which becomes particularly prominent when the cell starts migrating out of the tissue collective (modified from [12]).

Turing did not take into account any cell-mechanical aspects, although regenerating Hydra tissues, as well as other tissues, show distinct active mechanical movements. As a conclusion, we hypothesize that forces and movements are a crucial component for a stable regeneration of the organism.

It was shown that mechanical stress—under certain conditions—influences the chemical state of cells, e.g. β-catenin increases significantly on compression. Furthermore, β-catenin influences not only the regulation of the cytoskeleton but also the expression of genes well known from development and cancer [9–11]. However, the link to tissue fluctuations and movements is still to be explored.

Single cells revealed singular material properties, partially due to their highly dynamic polymer networks. The cytoskeleton built out of these polymers shows complex rheology partially depending on the mechanical past of the cell [13, 14]. This can now theoretically be captured [15–17]. Furthermore, the cell reacts specifically to mechanical stress with softening or stiffening dependent on the entanglement of the fibres and the time scale of observation (‘stiffening–softening paradox’) [18–20].

In most healthy grown tissues, cells usually neither strongly change shape nor migrate. However, it has been stated that tissue grafts lead to increased local cell motility [21] (epithelial mesenchymal transition (EMT)) and developmental gene activation (Wnt) [22] in Hydra organisms. In regenerating tissues cells equally show increased motility and Wnt-activity similar to single cells [23, 24]. It is plausible that this developmental gene may be related to cell motility and healing. Its relation to our findings remains to be studied.

What determines the large-scale ordering during regeneration and development? One mechanism was found by Holtfreter [25], who investigated embryonic tissues and suggested cell–cell affinity as a sorting mechanism. Foty and Steinberg showed the direct dependence of

surface tension on adhesion strength between cells in cellular aggregates ('differential adhesion hypothesis') analogous to demixing of immiscible fluids [26, 27]. Cell assemblies represent a unique material being able to switch between being fluid-like, solid-like or a material with mixed properties. Hydra tissues, as studied here, are extracted from adult animals and possess an extracellular matrix and stable inter-cellular junctions. In contrast to embryonic cell assemblies they rather behave like a soft solid material.

Fluctuations during Hydra regeneration have been investigated only rudimentarily so far [28–30] and only a few publications discuss fluctuations during morphogenesis for other species [31, 32]. It was found that tissue fragments and cellular aggregates always rearrange to spheroids (figure 1(b)). These spheroids show three phases of sawtooth-like semi-periodic fluctuations [28], which were found to be related to the expression pattern of a gene associated with the mechanical axis formation [33]. Fluctuations may be directly coupled to gene expression; however, many open questions remain.

In order to measure macroscopic shape changes with a high signal-to-noise ratio, fluorescent cells have been observed. Therefore, we used strains with eGFP (enhanced green fluorescent protein) being co-expressed along with β-actin in the epidermal as well as in the gastrodermal cells, and we studied them by confocal microscopy. As this β-actin was generally found to be uniformly expressed in our tissues, we used the variations in fluorescence intensity as an indicator of the deviation from the focal plane caused by tissue deformation.

Hydra cells also possess myoneme-like, force-generating actin structures (we assume α-actin) whereas cortical β-actin is rather involved in the control of stiffness and shape. Both systems are stabilized and dynamically restructured by motor proteins (myosins) and crosslinkers (e.g. actinin) [12]. However, we ignore the molecular scale, but concentrate our discussion on the principal functional subsystems: the mesoscopic filamentous structures called 'F-actin bundles/myonemes' and the 'β-actin'.

While we concentrate on the mechanical properties here, it is clear that the 'big picture' has to associate mechanics with signalling and genetic control. We expect that our findings are of general importance for biological pattern formation and complex systems and may lead to the unfolding of new medical approaches.

2. Folding dynamics

Fragments of different shapes were found to reshape into a spheroid in most cases. The tissue often rejects a larger number of cells during this folding process. The passage through the spheroidal state has been found without exception prior to the regeneration of a polyp; however, the reason for this necessity is not clear.

In order to obtain uniform and comparable temporal regeneration dynamics, we used toroids as an initial state (figure 2). This simple shape mimicks an infinite tissue for signal spreading and facilitates data analysis and the building of models. The dimensions of our toroidal cross-section are about $80 \times 140\,\mu$m (radial $\times$ coaxial direction) and $300\,\mu$m (overall diameter). The toroid's wall consists of a massive inner (gastrodermis) and a shell-like outer (epidermis) cell layer. The toroids comprise about 1500 ± 500 cells in total and for this arrangement we found the regeneration to a small polyp to be reproducible in about 80% of our experiments. In the remaining cases we did not observe folding. Instead the tissue just contracted until the inner aperture was closed or the toroid disintegrated completely. In the case of too small sections the folding still occurs but the reproduction probability of the polyp is

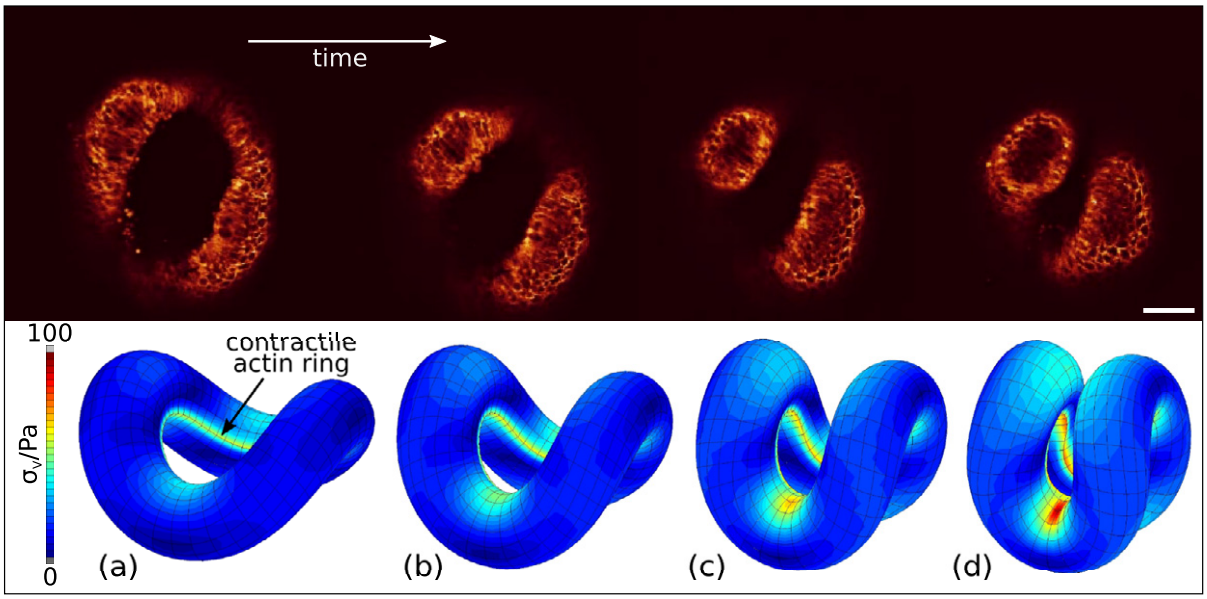

Figure 2. (a)–(d) The Hydra folding process (bar: 100 μm) as observed with confocal microscopy (upper row) and as a simulation (lower row). The confocal images show only a horizontal cross-section of the three-dimensional (3D) structure. In the results of the simulation (discussed in section 5) the location of the inner actin ring (toroid diameter 300 μm and cross section diameter 90 μm) is indicated by the increase of stress along the inner circumference of the toroid due to myosin–actin contraction. The vertically arranged states correspond approximately.

reduced. Below sizes of 200–300 cells the regeneration fails [34]. Too large sections do not fold but stay tube-like and heal at both ends prior to regeneration. In that case the axis of the organism is presumably conserved.

The folding process in 90% of our observations requires not more than (120 ± 30) s from the planar ring shape to the folded ring. The folding was considered complete when the opposite loops got into contact. The observed time period is clearly too short for diffusive signalling across the toroid, especially as an appropriate control loop would need several passages of wave fronts of signalling molecules before a gradient obtains stability. Half of the perimeter accounts for at least 20 cells and free extra-cellular diffusion would disperse a signal in not less than 10 min to reach the opposite side [35].

During wing morphogenesis of the fruit-fly a decapentaplegic (Dpp) morphogen intracellular gradient expansion speed of 6 μm in 5 h (this corresponds to 3 days to cross a Hydra toroid) has been measured [36], which is far too slow to explain Hydra toroid folding. Gene expression would also need many hours [37–39]. A sufficient control of diffusion based on gradients outside the tissue can hardly be imagined. In addition, the Hydra polyp lives in an aqueous environment which would strongly perturb such gradients.

Hydra possesses a primitive neuronal system mainly concentrated in the hypostome and peduncle region [40]. The toroids are taken from the centre of the gastric column, which is only sparsely populated with neurons. As most of their connections are destroyed during dissection, we assume that their contribution to the control of the folding process is at best marginal.

Other signal paths are provided by gap junctions, prominent for cardiomyocytes but still unknown for Hydra. They allow for a direct and extremely fast intercellular signal exchange based on electrical potential differences driving ion flow [41]. However, an organizer such as the sinoatrial node for the heart would be required to provide timing stability. Such a system is unknown in Hydra and, even if it existed, would presumably be negligible in our toroids.

Osmotic pressure of the gastrodermal cells as a possible origin of contraction and deformation can be excluded since the enteron (the inner cavity of a closed Hydra tissue) is hyperosmotic. This would result in a cellular swelling and not a contraction once these cells are exposed to the external medium [42].

These reasons support our conclusion that the gastrodermal cells are the force-generating cell type. Mechanical stress-relaxation waves propagate at the speed of sound and provide a means of very fast signal transmission. The corresponding speed $v = \sqrt{G/\rho}$ is in the range of about $0.1\,\mathrm{m\,s^{-1}}$ when assuming a shear modulus of $G \approx 100\,\mathrm{Pa}$ (soft cells; stiffer cells lead to even higher velocities) and a net tissue density $\rho \approx 1\,\mathrm{g\,ml^{-1}}$ [43]. Mechanical waves cross Hydra rings in milliseconds. The shear modulus is mainly controlled by the cellular cortex, which stabilizes cellular shape against external mechanical stress and osmotic pressure [42].

During the folding process, the gastrodermal cells in the fold are submitted to considerable compression, leading to strong deformation. In some cases this deformation results in a local tissue disassembly as some cells start migrating individually first, then they round up, their β-actin related fluorescence is strongly increased and, finally, some quit the tissue. This process resembles the EMT, which also plays a role in tumours and inflammation, for stem cells and during embryogenesis [44–46]. To our knowledge, a purely mechanical triggering of this transition has not been described before.

Cells remaining tissue-bound show a low, constant and uniform β-actin activity, providing stiffness to ensure the stability of the cells and the tissue (fig 4(a)). Even for strongly deformed cells an increase of the corresponding fluorescence intensity cannot be stated as long as the cells remain tissue-bound. These observations agree with gene expression studies where the β-actin signal has been found to be constant enough to serve as a reference for normalization of gene expression measurements [47]. However, this statement has to be revised in some cases as we observed significantly higher activity of β-actin, once the cells switch from the 'tissue state' to the individual migrating state. As we did only observe exclusively tissue bound (low fluorescence) or migrating (strong fluorescence) cells, we suggest a two-state approach for future models.

3. The actin machinery

The α-actin system of Hydra forms super-cellular bundles in the epidermis (myonemes) as well as in the gastrodermis. They are able to span across as much as seven cells. One epidermal cell contains about seven to ten bundles. The bundles in the two cell layers are oriented orthogonally to each other and form a two-dimensional Cartesian coordinate system, which allows absorption as well as generating stress in any direction. This explains the impressive motility of the organism. The epidermal bundles are oriented coaxially to the Hydra body and the dissected-toroid axis, and they are positioned regularly with an average distance of 3–5 μm. The gastrodermal bundles follow the contour of the toroid, with strongly varying density. We observed strong bending and length fluctuations in both systems. The gastrodermal bundles are

much less pronounced than the epidermal bundles and usually appear more clearly, once the tissue is slightly stimulated mechanically.

Whereas the observed β-actin density did not display any specific dynamics during that process either in the gastrodermis or in the epidermis. The F-actin forms bright zones prior to the folding event. Initially, actin is scattered in the apical cortex of the irregularly shaped gastrodermal cells. In the course of time the actin structures become denser and get aligned to bundles (figures 4(b)–(d)). Finally, a dense and strong actin ring is formed along the inner side of the toroid and the cell's apical side is flattened to a smooth inner contour. This is presumably due to increasing internal mechanical stress reducing the surface roughness. It is conceivable that the bundling process itself is self-sustained and amplified by this stress along the curved geometry. Simultaneous to the bundle formation, we observed a decrease in fluorescence intensity of the cytoplasm, probably due to actin depletion.

The epidermis arches as a relatively thin layer over the outer bound of the gastrodermis, which is much more voluminous. Due to their orientation, the epidermal α-actin bundles cannot be directly responsible for the folding. We assume that one of their duties is rather to distribute the stress field generated by the contracting gastrodermal bundle ring over the entire toroid. This ensures stability and reproducibility of the described dynamics.

The epidermis covers as a relatively thin layer the voluminous gastrodermis and possesses a system of long and equidistant epidermal bundles (figure 7). Their length was observed to fluctuate between 10 and 80 μm with rates up to 150 $\mu\mathrm{m\,min}^{-1}$. Actin polymerization is clearly too slow to yield such rates; hence, myosin is assumed to be at the origin [48]. The gastrodermal tissue beneath is periodically compressed by these fluctuations which would explain the observed densification and orientation of the gastrodermal actin structure. These contractile forces are transmitted to the adjacent cell layer by the flexible and porous extracellular matrix network [49]. The *a priori* highly oriented epidermal bundles presumably determine the orientation of the gastrodermal bundles which in turn generate the mechanical stress expressed in transversal epidermal fluctuations. The gastrodermal system was observed to regularly fractionate again and split up between the epidermal contractions. So it is much less stable than the epidermal one which may allow it to be more adaptive with respect to external changes in stress and shape.

We hypothesize that the gastrodermal actin ring as seen in figures 4(b)–(d) and 6(b)–(c) is responsible for the folding process. This is supported by observing the effect of partially dissolving the gastrodermis by the application of cytochalasin—an actin polymerization inhibitor. Degradation of the gastrodermis results when doses above 20 $\mu\mathrm{mol}\,\ell^{-1}$ are applied for 10 min. The epidermis was observed to be less prone to degradation than the gastrodermis. In figure 3(c) it can be observed that the epidermis is significantly more curved in regions where some gastrodermal cells are still attached to the tissue.

4. Differential contraction and toroidal symmetry breaking

In order to perform the described folding process the cylindrical symmetry of the toroid has to be violated. Due to the contraction of the actin ring in the gastrodermis, the whole tissue experiences an internal stress gradient ('differential contraction') between the actin-ring-forming and other cells and the toroidal shape becomes unstable. Small randomly distributed irregularities ('critical fluctuations') may be amplified now. As a consequence, the

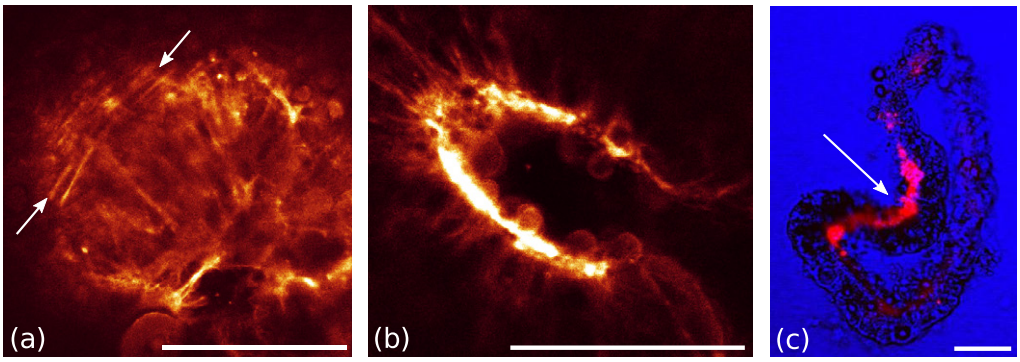

Figure 3. (a) The gastrodermal F-actin bundles are usually faint. However, if the fast deformation leads to an internal shear stress these structures are expressed more strongly (ends of bundles indicated by arrows). The folding axis is oriented horizontally. (b) During folding, the actin intensity is strongly increased on the apical side of the gastrodermal cells, indicating the contraction of this cell layer. (c) Cytochalasin at concentrations above 20 μmol ℓ^{-1} destroys the gastrodermis, whereas the epidermis seems to be more stable. Still some gastrodermal cells (red) remain intact in this picture. The curvature of the ring is more pronounced at that site (indicated by the arrow). This shows the crucial role of the gastrodermis in the folding process. All scale bars represent 100 μm.

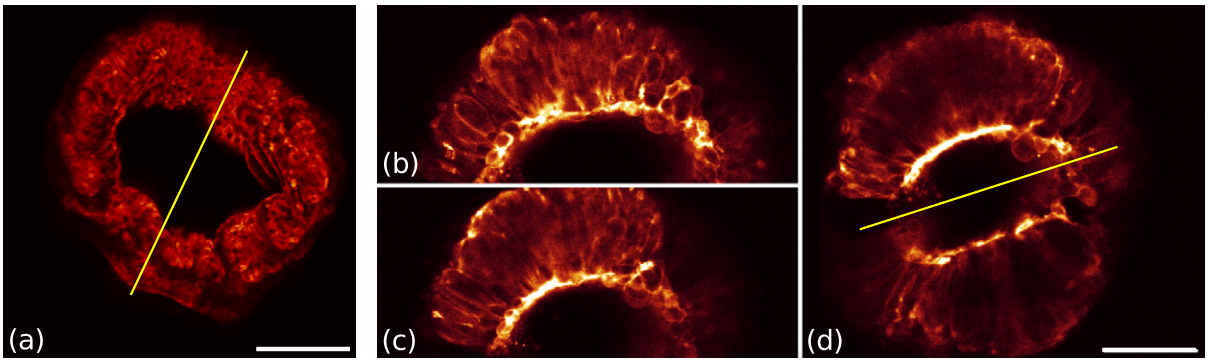

Figure 4. (a) The β-actin fluorescence intensity distribution in the gastrodermis of a projection of a partially folded (about 50%) Hydra toroid does not indicate the axis along which the folding occurs later (the axis in yellow). Therefore, we think that the folding axis selection is random. Panels (b)–(d) show a sequence of gastrodermal F-actin bundle formation in a later stage of the folding process. Initially (b), the actin is scattered over the apical sides of the cells. After about $2\frac{1}{2}$ min, (c) the bundle starts forming and at later times (d) it becomes straight and dense (the folding axis in yellow). All scale bars represent 100 μm.

tissue increases its curvature transversally and becomes wavy. The nature of the irregularities is not obvious, as thermal fluctuations are negligible at this length scale. The origin of these active fluctuations is presumably linked to the actin cytoskeleton which is known to be highly dynamic and a source of fluctuations [17].

Next, we attempt to relate single-cell mechanics to the described fluctuations of Hydra tissue toroids. The mechanics of single cells under different types of external forces and strains is currently being investigated extensively [14, 16, 50–54]. The spatial scale of these fluctuations was found to be larger than just a single cell; therefore, it presents a collective phenomenon.

During folding, cells are deformed strongly. This can lead to disassembly of the cytoskeletal actin crosslinkers. These crosslinkers are point-like and, therefore, concentrate the mechanical stress field strongly, which increases rupture probability. Therefore, even small strains (<10%) lead to an irreversible actin network rupture [14, 20]. The strain-softened cells extend and the overall stress is relaxed. However, the disrupted cytoskeletal structure of these cells reorganizes and stiffens slowly again after several minutes [14]. As the recovered stiffness exceeds the stiffness of the non-softened adjacent cells as can be seen in [14], the latter are stretched and shear-softened during a new folding trial. Therefore, repeated folding would occur along a varying axis. Indeed, we occasionally observed toroids to unfold and refold along different axes. Apparently, the toroids 'check out' if the folding was correct and repeat it on mismatch.

Cells actively react on stress. In preliminary experiments with toroids exposed to strong mechanical stress (2–5 μN) in a mechanical stretching device, we were unable to predict the position of rupture. α-actin was found to reinforce by bundling at the thinnest site presumably permitting the tissue to cope with the densified mechanical stress field. The active reinforcement of actin bundles in the gastrodermis protects the tissue from rupture.

The tissue fragment folds rapidly. When embedded in very soft agarose gel of concentrations from 0.2 to 1% [55], the folding onset can be retarded or stopped allowing for longer observation times. On a long term (about 1 h), we found three phases of the shape fluctuations—first a semi-periodic phase with typical frequencies in the range of 10 mHz, then a second phase with pulsations every few minutes and finally a silent phase. In the last phase the tissue organization starts to disintegrate partially (EMT).

Regarding the initial fluctuations leading to instability, we observed mainly creation and decay of stationary waves. Corresponding to the periodicity of the system we used discrete Fourier analysis of the fluorescence intensity along the toroid with the toroidal angle as a variable. We restricted our analysis to modes 2–15. Higher modes would account for sub-cellular deformations, which go beyond the scope of this paper. Modes 0 and 1 correspond to translation and rotation and, therefore, are irrelevant for the folding dynamics.

Our data are discussed only qualitatively as the described phenomena are reproducible, although not yet numerically. Initially, several of the lowest modes (2–10) were of about equal amplitude (see (iv) in figure 5(c)). At the time scale of several tens of minutes, all modes decayed with the exception of the second. This mode led directly to correct folding geometry. For stiffer gels we observed a reduction of excited modes and a slowing down of the dynamics. In an almost liquid 0.2% gel the second mode dominated after less than 5 min; in stiffer gels it needed significantly more time. Only in the stiffest gel (1%) the third mode was able to supersede the second in the end (see (iii) in figure 5(b)). This mode exchange can be explained by considering the distribution of the mechanical energy. We consider bending into the direction of the toroidal axis only and neglect modulations in the toroid plane. The bending energy of the toroid scales for excursion amplitudes a, which is small, like $E_{\mathrm{bend}} \sim a^2\, n^4$ (n is the mode number). In the gel-less case the energy is distributed equally among the modes according to the equipartition theorem. Then, the lowest modes dominate since $a \sim 1/n^2$. In linear approximation and assuming that the average force applied against the gel F is constant, the elastic energy of the gel is $E_{\mathrm{el}} \sim F^2/D$

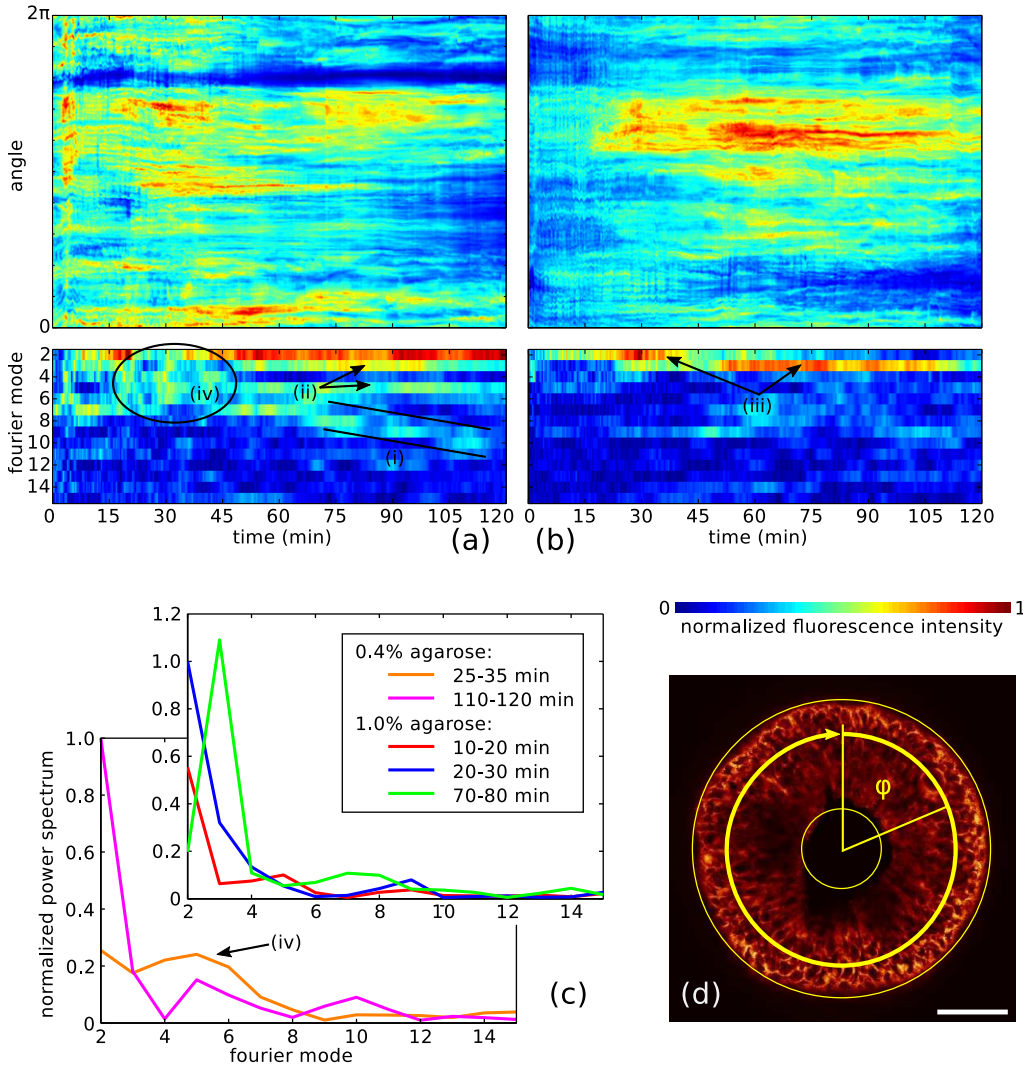

Figure 5. Hydra tissue in low melting agarose gel with concentrations of (a) 0.4, and (b) 1%. The gel inhibits the folding process and allows the long-term observation of the mode dynamics on the toroid. (a) Previous to the folding we found the presence of modes 2–7 with similar amplitudes. After a few minutes the higher modes disappear in favour of the second mode, finally leading to the folding process. We found a cascade dissipation mechanism (i) as well as the coupling of a number of even or odd modes (ii) reflecting even or odd mirror symmetry. In (b) the very stiff gel results in a winning third mode (iii). No higher modes are significant here. (c) Spectra, normalized with the initial value of the second mode and averaged over a short interval at the indicated times, are compared for the two gels: in the softer gel a block (2–6) of modes are of equal strength (iv) during the symmetry breaking (25–35 min), which decay later. Only the second mode survives and dominates finally. In stiffer gels no block could be seen; usually the second mode dominates during the transition. The presented case was observed in the stiffest gel: mode switching from the second to the

Figure 5. (Continued) third was found. The polyp was not able to be regenerated in this case. (d) A typical tissue ring with β-actin-labelled epidermis is shown together with the sampling strip along which the intensity was extracted and radially averaged for the Fourier analysis (bar: 100 μm).

(D is the elasticity constant) and the energy created by the contraction of the actin ring increases in time. The contraction process continuously delivers mechanical energy into the system being distributed between the gel and the bent toroid. However, the stiffer the gel is, the less energy it can store: $E_{\mathrm{el}} \sim 1/D$. Therefore, for stiffer gels the energy generated by the contraction goes preferably into the tissue deformation. Eventually, the even second mode is not absorptive enough anymore and the odd third mode is involved in taking over the excess energy, as the latter can store 5 times more energy compared to the second mode at equal excursion amplitudes ($E_{\mathrm{bend}} \sim n^4$) and dominates and suppresses the second mode by a still unknown nonlinear mode coupling.

The modes superior to the second one frequently decayed in a cascade through which their energy was progressively transferred to increasingly higher modes (a typical case is shown in (i) in figure 5(a)). This again can be explained by the better ability of higher modes to absorb the increasing amount of mechanical energy generated by the contracting actin ring. This might be a biological dissipation mechanism to transfer the steadily increasing energy from macroscopic to mesoscopic and possibly microscopic length scales, i.e. to the molecular level. The energy is completely transferred to the next higher mode, which indicates again a nonlinear competition of modes with different symmetries. We generally observed transient coupling of exclusively odd or even modes (a typical case is shown in (ii) in figure 5(a)). The modes of equal symmetries collaborate and modes of mixed symmetry compete. However, an explanation is still unavailable.

Finally, after a longer period when the folding process failed, cells round up, increase β-actin expression, form lamellipods and start migrating individually over the remaining tissue. We assume to have observed for the first time a purely mechanically triggered EMT.

5. Finite element simulations

In this section, we describe numerical simulations of the folding process using a 3D finite element model. The calculation assumes quasi-equilibrium and outputs the state as a function of the stress generated by the contractile actin ring.

In order to account for large deformations, an *updated Lagrangian formulation* [56] is chosen. The deformation behaviour is modelled by an Ogden material model of isotropic nonlinear elasticity [57–59], characterized by the free energy function $\psi(\lambda_k) = \sum_{I=1}^{n} \frac{\mu_I}{\alpha_I}(J^{-\frac{\alpha_I}{3}}(\lambda_1^{\alpha_I} + \lambda_2^{\alpha_I} + \lambda_3^{\alpha_I}) - 3) + g(J)$, with principal stretches λ_i, material parameters μ_I and α_I as well as n, the number of individual functions. The function $g(J)$ of the Jacobian $J = \lambda_1\lambda_2\lambda_3$ is used to model compressible material behaviour. Here, we use an Ogden formulation with $n = 1, \alpha_1 = 2$ and $g(J) = \frac{9K}{2}(J^{\frac{1}{3}} - 1)^2$, which is also known as a compressible Neo–Hooke material, where K is the bulk modulus. In the limit case of small strains this formulation reduces to linear elastic Hooke material. Regarding the material parameters, we chose a Young's modulus of $E = 100$ Pa and a Poisson's ratio of $\nu = 0.4$. The Poisson's ratio quantifies the negative ratio of transverse and longitudinal strain in a specimen undergoing

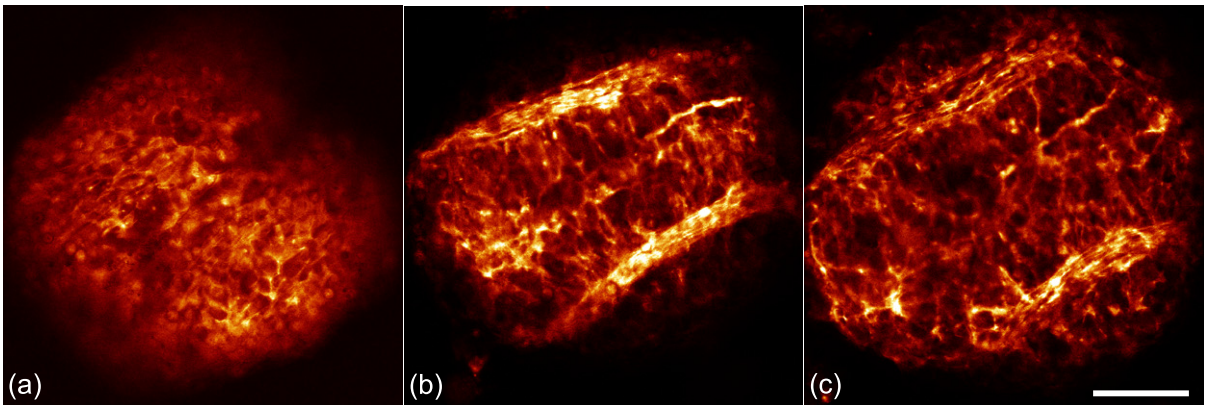

Figure 6. The actin ring seems to play an important role even in the already folded ring. Slight compression significantly amplifies this otherwise only hardly visible structure (a). The cells of the epidermis and the gastrodermis are pressed together and after half an hour (b) the cells in contact connect, inducing the closure of the gaps. Finally (c), the α-actin bundles start to disappear and a perfect spherical symmetry is established (bar: 100 μm). This spheroid, being symmetric in shape and mechanical properties (actin), is the starting point inevitable for the development of a novel organism.

uniaxial tension. The chosen number 0.4 allows for a small volume increase on extension, meaning that the material is assumed to be slightly compressible. From those parameters $\mu_1 = \frac{E}{2(1+\nu)}$ and $K = \frac{E}{3(1-2\nu)}$ can be calculated.

Tori with major radii of $R = 150\,\mu$m and varying minor radii r have been investigated. These were discretized by *hexahedral serendipity elements* with quadratic shape functions [60]. The inner actin ring, assumed to be responsible for the folding process, was modelled by linear truss elements. These are attached to the toroid along its inner circumference. To drive the folding process an increasing intrinsic strain was prescribed to the truss elements.

Simulations showed that numerical noise is not sufficient to break the symmetry of the toroid model. Thus, four equal additional forces distributed evenly around the toroid are applied, forcing the toroid slightly into the experimentally observed configuration. While reducing these additional forces back to zero, the simultaneously increasing intrinsic strain in the inner actin ring will keep the toroid in its bended shape. A further increase of the intrinsic strain then drives the folding. The here described process is adequate to prove the ability of the inner actin ring to fold the toroid if the initial condition describes a sufficiently bended configuration. We suggest that the active fluctuations described in section 4 serve to overcome this folding threshold.

Figure 2 features a toroid of 45 μm minor radius modelled by 2304 hexahedral and 96 truss elements. As the simulations show, the inner actin ring is able to fold the toroid, which proves the viability of our hypothesis. In figure 2(d) the inner ring exhibits tensile forces between about 50 and 150 nN. This results in a von Mises stress σ_V of up to about 100 Pa in the toroid. Thicker toroids did not succeed in folding but would rather return to their plane configuration when reducing the additional forces. This is to be expected, since for thick structures bending becomes less favourable compared to tension. Therefore, simulated toroids with aspect ratios $r/R > 0.3$ would rather tighten staying flat than deflect from their plane configuration, which we occasionally could also observe in our experiments.

The model is well suited to describing the observations qualitatively, whereas any numerical quantity values should be regarded as describing the order of magnitude of effects. Simplifications of the model are: ignoring the nature of the two cell layers as well as the presence of the extracellular matrix (mesoglea), the other actin structures, and finally, basing the simulation on a simple isotropic Ogden model. Furthermore, apart from the contractile actin ring we ignored active cellular reactions which modulate cellular stiffness and shape and which are presumably responsible for the described fluctuations.

6. Summary and conclusion

In the present paper, we studied regeneration of the cellular toroids of about 1500 *Hydra vulgaris* cells. The toroid geometry has been selected as it is the simplest one after spheroids, allowing for clean observation and analysis.

During the first phase of the regeneration process, cellular toroids composed of cells display a highly symmetric and unusually fast folding dynamics. After 2 min a compact form is achieved which transforms into a spheroid with a correct cellular bilayered structure.

In order to study the symmetry breaking, we embedded the toroids into gels of varying stiffnesses and analysed the modulation dynamics by circular Fourier decomposition. For soft gels, the second mode prevails that matches perfectly the folding geometry. For stiff gels, we observed a dominant third mode that is capable of accommodating more bending energy for a given amplitude. Energy transfer cascades to higher modes were also found for modes beyond the third order. The observed phases of exclusively excited even or odd modes indicate a symmetry-dependent interaction between modes of different order.

The subsequent folding process can be explained purely mechanically based on 'differential contraction': a subpopulation of cells in a tissue spontaneously contracts collectively, which leads to stress gradients and shape modulation of the tissue. At its origin we discovered an actin ring at the inner side of the toroid. In order to observe its creation we observed actin in embedded toroids as well as in stretched tissue (1–10 μN). The actin ring showed in both cases growth and strengthening. As a result actin creates stress, which, in turn, amplifies the actin structure, again presenting a self-organization process of the ring formation.

A numerical finite element model of stiff toroids with a tensile stress ring at the inner bound confirmed the mechanism: the ring contraction destabilizes increasingly the arrangement of the otherwise stable flat toroid. In addition, the simulation revealed properties that are not accessible experimentally: a deformation threshold has to be crossed in order to reproduce the observed toroid bending. The finite element simulation revealed further that the ratio between the cross section and the major diameter had to be below a critical value to accomplish folding. Otherwise the inner bound of the toroid only contracts without excursion into the third dimension. These findings imply that the fluctuations responsible for the transition have to pass a minimal amplitude in order to initiate the dynamics. We hypothesize, as thermal fluctuations are too small at this length scale, that this is the reason why cells and groups of cells actively consume energy to maintain strong enough fluctuations.

The folding was related to single cell dynamics. Tissue cells are put under stress by deforming neighbouring cells. Large enough deformation stress softens the cell, which stabilizes the folding site and reduces the folding force. The cells remain soft for several minutes after stress release (hysteresis) before re-gaining the natural parameters again. After recovery the

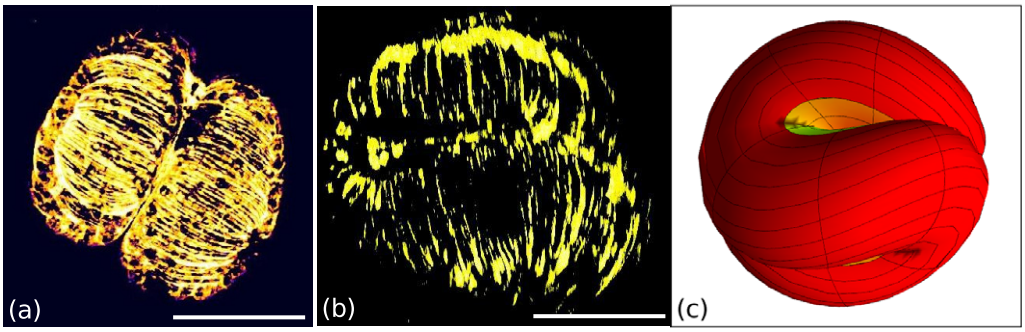

Figure 7. (a) Top view of the epidermal F-actin bundles (myonemes) which (b) builds arches over the gastrodermal loops (bars: 100 μm). The stiffness of these bundles stabilizes while providing enough flexibility to follow the transverse and longitudinal fluctuations due to the gastrodermal cells. The orientation of (b) is visualized in (c).

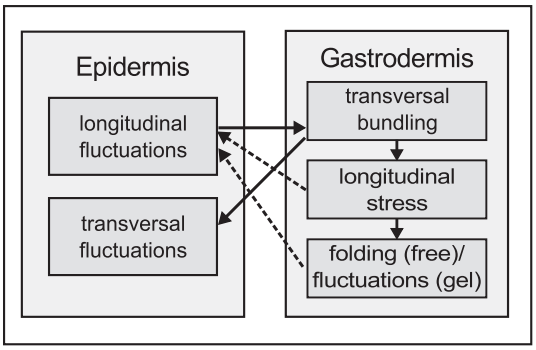

Figure 8. The scheme shows the hypothetical control dependences of the different actin systems. The fluctuations of the epidermal actin structure bundle the gastrodermal actin forming a ring. As a consequence the stress is increased, which leads to the folding process or to the transverse epidermal fluctuations as well as the tissue contractions when embedded in gel. We speculate that mechanical feedback (dashed lines) is responsible for synchrony and stability of the epidermal actin fluctuations.

stiffness reinforcement was observed to overshoot the previous value [14]: this favours the tissue to fold at different sites depending on the recovery time.

The epidermis provides equidistant F-actin stripes capable of stabilizing the large-scale structure (figures 7(a) and (b)). We found fast longitudinal myosin-driven fluctuations. As we found, these fluctuations bundle and reinforce the perpendicularly oriented gastrodermal actin fibres forming the contractile actin ring. The gastrodermal layer also shows contracting fluctuations, which, in turn, are expressed as transverse fluctuations of the epidermal actin structure. This cross coupling of fluctuations across the mesoglea may present a mechanical closed control loop organizing the described folding so perfectly (figure 8). In the end state of folding, the outermost cells join until a double layered spotless spheroid is obtained. This is the starting point of the morphogenesis of a new Hydra as described elsewhere.

The long-term observation of tissue toroids in gels revealed a purely mechanically induced transition to individual cellular behaviour (EMT). The tissue bound cells evade and migrate as individuals over the remaining tissue. We also observed the inverse process (mesenchymal epithelial transition), i.e. migrating cells penetrate the tissue again and re-integrate. The β-actin level in the migrating state was observed to be significantly increased in contrast to the actin fluorescense signal. The cells seem to possess two clearly distinct states. A future theoretical model may take this into account and may be based on corresponding transition rates. However, the phenomenon remains to be investigated more deeply.

7. Materials and methods

We cultivate four transgenic *Hydra vulgaris* strains with fluorescence labelled epithelial–muscle cells either for the gastrodemis or the epidermis. Two cultures are transfected with the F-actin-binding Lifeact peptide [61], whereas the other two cultures express eGFP with a β-actin promoter and terminator [62] simultaneously to the functional β-actin of the cells. Therefore, the eGFP signal quantifies the β-actin concentration. All strains are kept in crystallizing dishes in our chemistry laboratory at temperatures of $(18 \pm 1)\,^{\circ}$C. All cultures are fed with freshly hatched *Artemia salina nauplii* once a day and the medium is changed 3–5 h after feeding. Our medium is composed of 1.0 mmol ℓ^{-1} $CaCl_2$, 0.1 mmol ℓ^{-1} $MgCl_2$, 0.03 mmol ℓ^{-1} KNO_3, 0.5 mmol ℓ^{-1} $NaHCO_3$ and 0.08 mmol ℓ^{-1} $MgSO_4$ in Millipore water.

The rings were obtained by dissecting the tissue from the central gastric column and immediately transferred to a modified petri dish with a 170 μm coverslip mounted over an aperture and with a polytetrafluorethylene plate containing holes with a diameter of 1 mm. The teflon plate suppresses parasitic convective flow carrying the Hydra rings out of the observation field. The chamber was filled with either medium- or low-temperature melting agarose gel (Sigma-Aldrich A0701) and all together was completely submerged in Hydra medium to avoid osmotic and concentration changes due to evaporation.

The toroids were observed on a Leica DM IRE2 inverted microscope coupled with a Leica TCS SP2 AOBS confocal scanner and a Leica HC PL Fluotar 10×/0.30 objective.

The toroids were made from polyps starved for 24 h and selected for healthy shape prior to dissection. A double-blade scalpel was used to cut out the segments. With this technique, we avoid large thickness variations due to polyp contractions. As the tissue movements are considerable during the first 30 s the toroid had to be transferred fast to the observation platform.

The images were visualized and analysed with ImageJ 1.45s and in-house-developed Mathematica 8.0 and MatLab R2011a scripts.

For the gastrodermal tissue degradation Cytochalasin D (Sigma-Aldrich C8273) was applied at concentrations up to 20 μmol ℓ^{-1} for 10 min. The petri dish was gently shaken for 10 s before observation.

The finite element simulations were done using Marc Mentat 2010.1.0. One calculation for the chosen resolution took about 1 h.

Acknowledgments

The work presented in this paper was made possible by funding from the German Federal Ministry of Education and Research (BMBF; PtJ-Bio, 0315883). We are indebted to Josef Käs, Klaus Kroy and Matti Gralka (Leipzig), Thomas Bosch and Konstantin Khalturin (Kiel), Bert

Hobmayer (Innsbruck), Albrecht Ott (Saarbrücken) and Roland Aufschnaiter (München) for many discussions and for providing us with materials, especially the transgenic Hydra strains, as well as giving us access to confocal microscopy. We are also grateful for support from Magna Diagnostics GmbH (Leipzig).

References

[1] Martínez D E 1998 Mortality patterns suggest lack of senescence in Hydra *Exp. Gerontol* **33** 217–25
[2] Wetzel G 1895 Transplantationsversuche mit Hydra *Arch. f. mikr. Anat.* XLV
[3] Hefferan M 1901 Experiments in grafting Hydra *Arch. f. Entw.-Mech. d. Org.* **13** 4 565–87
[4] Mutz E 1930 Transplantationsversuche an Hydra mit besonderer Berücksichtigung der Induktion, Regionalität und Polarität *Dev. Genes Evol.* **121** 210–71
[5] Turing A M 1952 The chemical basis of morphogenesis *Phil. Trans. R. Soc.* **237** 37–72
[6] Gierer A and Meinhardt H 1972 A theory of biological pattern formation *Kybernetik* **12** 30–9
[7] Meinhardt H and Gierer A 2000 Pattern formation by local self-activation and lateral inhibition *Bioessays* **22** 753–60
[8] Bode H R 2009 Axial patterning in Hydra *Cold Spring Harb. Perspect. Biol.* **1** a000463
[9] Whitehead J, Vignjevic D, Fütterer C, Beaurepaire E, Robine S and Farge E 2008 Mechanical factors activate beta-catenin-dependent oncogene expression in apc mouse colon *Human Front. Sci. Program J.* **2** 286–94
[10] Fletcher D A and Dyche R Mullins 2010 Cell mechanics and the cytoskeleton *Nature* **463** 485–92
[11] Farge E 2011 Mechanotransduction in development *Curr. Top. Dev. Biol.* **95** 243–65
[12] Gunning P, Weinberger R and Jeffrey P 1997 Actin and tropomyosin isoforms in morphogenesis *Anat. Embryol. (Berl.)* **195** 311–5
[13] Fernández P and Ott A 2008 Single cell mechanics: stress stiffening and kinematic hardening *Phys. Rev. Lett.* **100** 238102
[14] Trepat X, Deng L, An S S, Navajas D, Tschumperlin D J, Gerthoffer W T, Butler J P and Fredberg J J 2007 Universal physical responses to stretch in the living cell *Nature* **447** 592–5
[15] Wolff L, Fernandez P and Kroy K 2010 Inelastic mechanics of sticky biopolymer networks *New J. Phys.* **12** 053024
[16] Janmey P A and McCulloch C A 2007 Cell mechanics: integrating cell responses to mechanical stimuli *Annu. Rev. Biomed. Eng.* **9** 1–34
[17] Wen Q and Janmey P A 2011 Polymer physics of the cytoskeleton *Curr. Opin. Solid State Mater. Sci.* **15** 177–82
[18] Wang N, Tolić-Nørrelykke I M, Chen J, Mijailovich S M, Butler J P, Fredberg J J and Stamenović D 2002 Cell prestress. I. stiffness and prestress are closely associated in adherent contractile cells *Am. J. Physiol. Cell Physiol.* **282** C606–16
[19] Park C Y, Tambe D, Alencar A M, Trepat X, En Hua Zhou, Millet E, Butler J P and Fredberg J J 2010 Mapping the cytoskeletal prestress *Am. J. Physiol. Cell Physiol.* **298** C1245–52
[20] Wolff L, Fernández P and Kroy K 2012 Resolving the stiffening–softening paradox in cell mechanics *PLoS One* **7** e40063
[21] Fujisawa T, David C N and Bosch T C 1990 Transplantation stimulates interstitial cell migration in Hydra *Dev. Biol.* **138** 509–12
[22] Chera S, Ghila L, Wenger Y and Galliot B 2011 Injury-induced activation of the mapk/creb pathway triggers apoptosis-induced compensatory proliferation in Hydra head regeneration *Dev. Growth Differ.* **53** 186–201
[23] Hobmayer B, Rentzsch F, Kuhn K, Happel C M, von Laue C C, Snyder P, Rothbächer U and Holstein T W 2000 Wnt signalling molecules act in axis formation in the diploblastic metazoan Hydra *Nature* **407** 186–9
[24] Galliot B and Ghila L 2010 Cell plasticity in homeostasis and regeneration *Mol. Reprod. Dev.* **77** 837–55
[25] Holtfreter J 1939 Gewebeaffinität, ein Mittel der embryonalen Formbildung *Arch. f. Experimentelle Zellforschung* **23** 169–209

[26] Foty R A and Steinberg M S 2004 Cadherin-mediated cell–cell adhesion and tissue segregation in relation to malignancy *Int. J. Dev. Biol.* **48** 397–409
[27] Foty R A and Steinberg M S 2005 The differential adhesion hypothesis: a direct evaluation *Dev. Biol.* **278** 255–63
[28] Fütterer C, Colombo C, Jülicher F and Ott A 2003 Morphogenetic oscillations during symmetry breaking of regenerating *Hydra vulgaris* cells *Europhys. Lett.* **64** 137–43
[29] Soriano J, Colombo C and Ott A 2006 Hydra molecular network reaches criticality at the symmetry-breaking axis-defining moment *Phys. Rev. Lett.* **97** 258102
[30] Kosevich I A 2006 Mechanics of growth pulsations as the basis of growth and morphogenesis in colonial hydroids *Ontogenez* **37** 115–29
[31] Koth S, Krahe M and Fütterer C 2011 Fluctuations and symmetries in biology and physics *Cell News* **4** 41–6
[32] Solon J, Kaya-Copur A, Colombelli J and Brunner D 2009 Pulsed forces timed by a ratchet-like mechanism drive directed tissue movement during dorsal closure *Cell* **137** 1331–42
[33] Soriano J, Rüdiger S, Pullarkat P and Ott A 2009 Mechanogenetic coupling of Hydra symmetry breaking and driven turing instability model *Biophys. J.* **96** 1649–60
[34] Shimizu H, Sawada Y and Sugiyama T 1993 Minimum tissue size required for Hydra regeneration *Dev. Biol.* **155** 287–96
[35] Francis K and Palsson B O 1997 Effective intercellular communication distances are determined by the relative time constants for cyto/chemokine secretion and diffusion *Proc. Natl Acad. Sci. USA* **94** 12258–62
[36] Entchev E V, Schwabedissen A and González-Gaitán M 2000 Gradient formation of the TGF-beta homolog DPP *Cell* **103** 981–91
[37] Noble K N and Wente S R 2010 Nuclear mRNA on the move *Nature Cell Biol.* **12** 525–7
[38] Cheadle C, Fan J, Cho-Chung Y S, Werner T, Ray J, Do L, Gorospe M and Becker K G 2005 Stability regulation of mRNA and the control of gene expression *Ann. NY Acad. Sci.* **1058** 196–204
[39] Fan J, Zeller K, Chen Y-C, Watkins T, Barnes K C, Becker K G, Dang C V and Cheadle C 2010 Time-dependent c-myc transactomes mapped by array-based nuclear run-on reveal transcriptional modules in human b cells *PLoS One* **5** e9691
[40] Grimmelikhuijzen C J, Dockray G J and Schot L P 1982 Fmrfamide-like immunoreactivity in the nervous system of Hydra *Histochemistry* **73** 499–508
[41] McDowall A W and Grimmelikhuijzen C J 1980 Intercellular junctions in nerve-free Hydra *Cell Tissue Res.* **209** 217–24
[42] Kücken M, Soriano J, Pullarkat P A, Ott A and Nicola E M 2008 An osmoregulatory basis for shape oscillations in regenerating Hydra *Biophys. J.* **95** 978–85
[43] Orescanin M, Qayyum M A, Toohey K S and Insana M F 2009 Complex shear modulus of thermally-damaged liver *Proc. IEEE Ultrason. Symp.* 127–30
[44] Zhao R, Wu Z and Zhou Q 2011 Epithelial-mesenchymal transition and tumor metastasis *Zhongguo Fei Ai Za Zhi* **14** 620–4
[45] Dave B, Mittal V, Tan N M and Chang J C 2012 Epithelial-mesenchymal transition, cancer stem cells and treatment resistance *Breast Cancer Res.* **14** 202
[46] Holley S A 2007 The genetics and embryology of zebrafish metamerism *Dev. Dyn.* **236** 1422–49
[47] Ferguson R E, Carroll H P, Harris A, Maher E R, Selby P J and Banks R E 2005 Housekeeping proteins: a preliminary study illustrating some limitations as useful references in protein expression studies *Proteomics* **5** 566–71
[48] Kuhn J R and Pollard T D 2005 Real-time measurements of actin filament polymerization by total internal reflection fluorescence microscopy *Biophys. J.* **88** 1387–402
[49] Shimizu H, Aufschnaiter R, Li L, Sarras M P Jr, Borza D-B, Abrahamson D R, Sado Y and Zhang X 2008 The extracellular matrix of Hydra is a porous sheet and contains type iv collagen *Zoology (Jena)* **111** 410–8
[50] Angelini T E, Hannezo E, Trepat X, Fredberg J J and Weitz D A 2010 Cell migration driven by cooperative substrate deformation patterns *Phys. Rev. Lett.* **104** 168104

[51] Lin Y-C, Tambe D T, Park C Y, Wasserman M R, Trepat X, Krishnan R, Lenormand G, Fredberg J J and Butler J P 2010 Mechanosensing of substrate thickness *Phys. Rev.* E **82** 041918
[52] Klein E A, Yin L, Kothapalli D, Castagnino P, Byfield F J, Xu T, Levental I, Hawthorne E, Janmey P A and Assoian R K 2009 Cell-cycle control by physiological matrix elasticity and *in vivo* tissue stiffening *Curr. Biol.* **19** 1511–8
[53] Tee S-Y, Bausch A R and Janmey P A 2009 The mechanical cell *Curr. Biol.* **19** R745–8
[54] Tee S-Y, Fu J, Chen C S and Janmey P A 2011 Cell shape and substrate rigidity both regulate cell stiffness *Biophys. J.* **100** L25–7
[55] Normand V, Lootens D L, Amici E, Plucknett K P and Aymard P 2000 New insight into agarose gel mechanical properties *Biomacromolecules* **1** 730–8
[56] Belytschko T, Liu W K and Moran B 2000 *Nonlinear Finite Elements for Continua and Structures* (New York: Wiley)
[57] Ogden R W 1972 Large deformation isotropic elasticity-correlation of theory and experiment for incompressible rubberlike solids *Proc. R. Soc. Lond.* **326** 565–84
[58] Ogden R W 1972 Large deformation isotropic elasticity—correlation of theory and experiment for compressible rubberlike solids *Proc. R. Soc. Lond.* **328** 567–83
[59] Simo J C and Taylor R L 1991 Quasi-incompressible finite elasticity in principal stretches: continuum basis and numerical algorithms *Comput. Methods Appl. Mech. Eng.* **85** 273–310
[60] Cook R D 2001 *Concepts and Applications of Finite Element Analysis* (New York: Wiley)
[61] Riedl J *et al* 2008 Lifeact: a versatile marker to visualize F-actin *Nature Methods* **5** 605–7
[62] Wittlieb J, Khalturin K, Lohmann J U, Anton-Erxleben F and Bosch T C G 2006 Transgenic Hydra allow *in vivo* tracking of individual stem cells during morphogenesis *Proc. Natl Acad. Sci. USA* **103** 6208–11